THE PENNSYLVANIA STATE UNIVERSITY
SCHREYER HONORS COLLEGE

DEPARTMENT OF CIVIL AND ENVIRONMENTAL ENGINEERING

RADIUM ACCUMULATION IN SEDIMENT ASSOCIATED WITH COAL DRAINAGE: DEPENDENCE ON ENVIRONMENTAL CONDITIONS AND SEQUESTRATION MECHANISMS

GARRETT EDWARD REESE
SPRING 2020

A thesis
submitted in partial fulfillment
of the requirements
for a baccalaureate degree in Chemical Engineering
with honors in Environmental Engineering

Reviewed and approved* by the following:

John Regan
Professor of Environmental Engineering
Thesis Honors Advisor

Nathaniel Warner
Professor of Civil and Environmental Engineering
Head of Environmental Engineering Undergraduate Minor
Thesis Supervisor

Andrew Zydney
Senior Professor of Chemical Engineering
Honors Adviser

* Electronic approvals are on file.

ABSTRACT

The objective of this thesis was to explore and document the levels of radium activity present at several different coal mining discharge sites in both western and eastern Pennsylvania. More specifically, the scope of this thesis was to observe how the environmental conditions of Pennsylvania's coal regions, which consisted of either anthracite or bituminous coal mining, affect the sequestration mechanism of radium. Due to a rich past of coal mining in these areas, thousands of miles of streams were left polluted with acid mine drainage (AMD), which contains high levels of sulfate, manganese, and iron oxides. In these regions, radium would likely be adsorbed by manganese and iron oxides as opposed to the common mechanism of co-precipitation with barium and sulfate as radiobarite. If radium is adsorbed and not co-precipitated as radiobarite, radium could be mobilized downstream of discharges. Thus, by sampling regions rich in sulfate, manganese and iron oxide minerals, such as those affected by AMD, this hypothesis was tested. Anthracite samples that were subjected to a four-step sequential leaching process had only two samples that maintained all radium after the first three steps that target soluble salts, exchangeable cations, and carbonates. These samples, Tracy Wetland and Silvercreek Out, had concentrations of 0.90 and 1.69 ppm for manganese and 2.99 and 0.15 ppm for iron respectively. Their corresponding barium concentrations were 0.046 and 0.038 ppm respectively. Given these values, it is assumed that both samples would have a majority of the radium removed after the final leaching step that targets iron and manganese oxides. All bituminous samples (Sterrett 1, Sterrett 2, Sterrett 3, and Sterrett Flush) maintained most of the initial radium through the first three steps of the sequential leaching process and collectively had higher concentrations of manganese and iron when compared to barium. Iron concentrations

were approximately 0.17 ppm while the manganese concentrations were quite higher at 1.1 ppm. However, the concentrations of barium in bituminous samples were exceptionally low at 0.013 ppm. Overall, it is likely that both anthracite and bituminous sample sets would lose most of their adsorbed radium after the fourth and final leaching step. If this were true, then it would prove that radium would adsorb to iron and manganese oxides in coal regions of Pennsylvania instead of the typical route of co-precipitating with barium and sulfate as radiobarite. Once this final leaching step is completed in the near future, these speculations can be verified.

TABLE OF CONTENTS

LIST OF FIGURES

LIST OF TABLES

ACKNOWLEDGEMENTS

This research project could not have been successful if it were not for the collective efforts of Bonnie McDevitt, Dr. Nathaniel Warner, and Malichai Jones. Likewise, Charles Cravotta has been an incredibly helpful benefactor for locating and gathering samples throughout Pennsylvania. None of the data featured throughout this thesis would have been readily available to our team had Charles not provided us with the necessary information required to obtain samples.

Chapter 1 – Introduction

Acid Mine Drainage Background and Definition

Over the course of the last 200 years, coal deposits in Pennsylvania have been greatly exploited as a source of fuel for both industrial and domestic use[1]. Due to the sheer abundance of coal mining operations in Pennsylvania's past, there are currently over 3,000 miles of rivers and streams contaminated with acidic overflow from the remanence of abandoned mines. This alone represents a third of the overall abandoned mine related pollution in the United States, and causes over 67 million dollars in lost sport fishing revenue each year due to the degradation of aquatic environments imposed by acid mine drainage[1]. The Pennsylvania Department of Environmental Protection estimated that it would cost approximately 20 billion dollars to completely remediate all sections of Pennsylvania's watersheds affected by acid mine drainage[1].

Acid mine drainage (AMD) is simply defined as the overflow of acidic water from abandoned mines, with coal mines specifically being the most common source in Pennsylvania[4]. Fresh water typically has a neutral pH of 7, yet water affected by AMD may have a variety of different pH values ranging from 2.7 to 7.3 as determined by a subset of 140 discharge samples taken from both anthracite and bituminous regions of PA[1]. AMD is characterized by high levels of heavy metals such as iron, aluminum, and manganese with the most prominent trace metals being Zn, Ni, Co, Ti, Cr, Pb, Cd, and Cu[1]. AMD also contains elevated concentrations of certain metalloids, with arsenic typically being of greatest concern[2].

The weathering of sulfide minerals results in a majority of the surface water and groundwater contamination associated with mining operations. Iron disulfide, or pyrite, is

principally responsible for the generation of acidic discharges from abandoned mines. The initial reaction that results in the formation of AMD involves the breakdown of pyrite in the presence of oxygen and water to yield ferrous iron, sulfate, and acidity[4]. The primary chemical reaction for the oxidation of pyrite is shown in Reaction 1 below:

$$4\,FeS_2 + 14\,O_2 + 4\,H_2O \longrightarrow 4\,Fe^{2+} + 8\,H^+ + 8\,SO_4^{2-} \quad (1)$$

The rate limiting step of the overall sequence is defined by the oxidation of ferrous iron (Fe^{2+}) to ferric iron (Fe^{3+}) that occurs following the breakdown of pyrite. Ferrous iron in the presence of oxygen and acid yields ferric iron and water via Reaction 2 as follows:

$$4\,Fe^{2+} + O_2 + 4\,H^+ \longrightarrow 4\,Fe^{3+} + 2\,H_2O \quad (2)$$

Once ferrous iron is oxidized, the resulting ferric iron is hydrolyzed to produce solid ferric hydroxide ($Fe(OH)_3$) with the addition of more acid. This step is dependent on pH where the solid mineral will not form with a pH less than 3.5 but will precipitate once a pH of 3.5 or greater is met. Once the appropriate pH conditions are reached, Reaction 3 will occur as shown:

$$Fe^{3+} + 3H_2O \longrightarrow Fe(OH)_3 + 3\,H^+ \quad (3)$$

Ferric hydroxide is associated with the infamous dark orangish red tint that is a clear indication of AMD pollution[4]. As the acidity increases, Reaction 3 is bound to begin a rapid cyclic propagation of acid generation by ferric iron, driven by the pH restriction discussed above, until the supply is depleted. The overall sequence of reactions produces a net flux of acid that is summarized in Reaction 4. (4)

$$4\,FeS_2 + 15\,O_2 + 14\,H_2O \longrightarrow 4\,Fe(OH)_3 + 8\,H_2SO_4$$

Pyrite + Oxygen + Water → Ferric Hydroxide + Sulfuric Acid

Figure 1: Abandoned mine discharge in Hegins, Pennsylvania.

Treatment Options for Acid Mine Drainage

There are several methods available for treating acid mine drainage. The options are divided into two categories: abiotic systems that utilize chemicals to neutralize and separate out heavy metals, and biological systems that use natural methods to filter AMD[2]. Regardless, both abiotic and biological systems can be classified as either passive or active depending on the amount of input required during operation. Active systems require continuous input of neutralizing agents and monitoring to sustain the process whereas passive systems need little to no input once the operation begins. Common forms of abiotic treatment involve the active introduction of oxygen and lime into waterways affected by AMD that require constant replenishment of O_2 and lime in order to function properly. Biological systems usually consist of passive aerobic wetlands, compost reactors, permeable reactive barriers, and packed bed bioreactors that simply treat acidic water as it flows through with minimal monitoring[2].

The most common form of treatment is active abiotic treatment, or chemical neutralization, which involves adding chemicals to the source of AMD in an attempt to alter the pH and promote the precipitation of heavy metals[4]. This method is not particularly efficient for the calcium carbonate (limestone) used to raise the pH is not cheap and neither is it effective when the levels of iron are extremely high[4]. Passive treatment, which has recently been in the spotlight for treating acid mine drainage, pertains mostly to using aerobic wetlands to essentially remove metals via absorption, consumption, and filtration by wetland plants such as cattails. Likewise, common passive treatment options extend to using anaerobic wetlands made of things such as manure and sawdust to promote anaerobic bacterial activity that ultimately results in the precipitation of metal sulphides with the generation of bicarbonate alkalinity[4].

Associated Radium Background

Radium is a radioactive alkaline earth metal found naturally in low concentrations throughout various environments[5]. Despite its natural origins, radium is associated with increasing cancer risks especially when given the ability to accumulate into higher concentrations in drinking water[5]. High concentration of radium can also be correlated to increases in cases involving lymphoma, bone cancer, and leukemia[3]. The two isotopes of interest, ^{226}Ra and ^{228}Ra, are particularly harmful due to their persistence in natural ecosystems with half-lives of 1600 and 5.75 years respectively. Radium-226 stems from the parent rock material uranium-228 while radium-228 originates from the parent rock material thorium-232[3]. The US Environmental Protection Agency determined a maximum safe concentration of 5 pCi/L for combined radium (the sum of ^{226}Ra and ^{228}Ra) in public drinking water supplies.

Radium is typically expected to naturally adsorb with other alkaline earth cations. Specifically, radium can be found in its aqueous form (Ra^{2+}, $RaOH^{+}$, $RaCl^{+}$, $RaCO_3^0$, or $RaSO_4^0$) within freshwater aquifers and associated surface waters adsorbed to minerals such as iron oxide, manganese oxide, clays, organic matter, barite, celestite, witherite, or strontianite[5]. However, the most common co-precipitation of radium occurs with barite and celestite when in the presence of sulfate to form radiobarite (Ba, Ra)SO_4 and radiocelestite (Sr, Ra)SO_4 when compared to co-precipitation methods with supersaturated carbonate minerals[5].

While previous studies have found that radium typically co-precipitates with barium and celestite in nature, this study aims to examine the optimal sequestration mechanism for radium when introduced to high levels of minerals associated with acid mine drainage such as iron oxides and manganese oxides. No previous studies have been published regarding the accumulation of radium in coal regions of PA and how these induced environmental conditions affect sequestration mechanisms. Likewise, the effects of passive versus active treatment systems has not been previously observed in regard to sequestration mechanisms involving the co-precipitation of radium.

Chapter 2 – Materials and Methods

Field Water and Sediment Sampling

Sediment (n=23) and water samples (n=21) were collected across two separate sampling events (January and April 2019). Bituminous samples from western Pennsylvania were obtained in January of 2019 while the anthracite samples were taken in April of 2019. Eight water samples and ten sediment samples were taken from various active lime treatment systems in the Pittsburgh region. An additional 13 anthracite water and sediment samples and were gathered in eastern Pennsylvania containing primarily untreated discharges along with four samples from passive treatment systems referred to in this document as "Otto out," "Silvercreek Out," "Silvercreek Cell 3 Out," and "Tracy Wetland."

Figure 2: Garrett Reese with USGS researcher, Charles Cravotta, gathering sediment samples in eastern PA.

Field measurements of pH, temperature, dissolved oxygen, oxygen reduction potential (ORP), and specific conductance were collected at each sampling point. Water samples were filtered with a 0.45-micron cellulose acetate filter and stored in lab refrigeration units at 4 degrees Celsius. Samples prepared for cation analysis were preserved with nitric acid to a pH less than or equal to 2. Samples dedicated exclusively to anion analysis were not preserved. All sediment samples (3 per site) were taken from the top 5 centimeters of soil. The distribution of samples sites is shown in Figure 2 below.

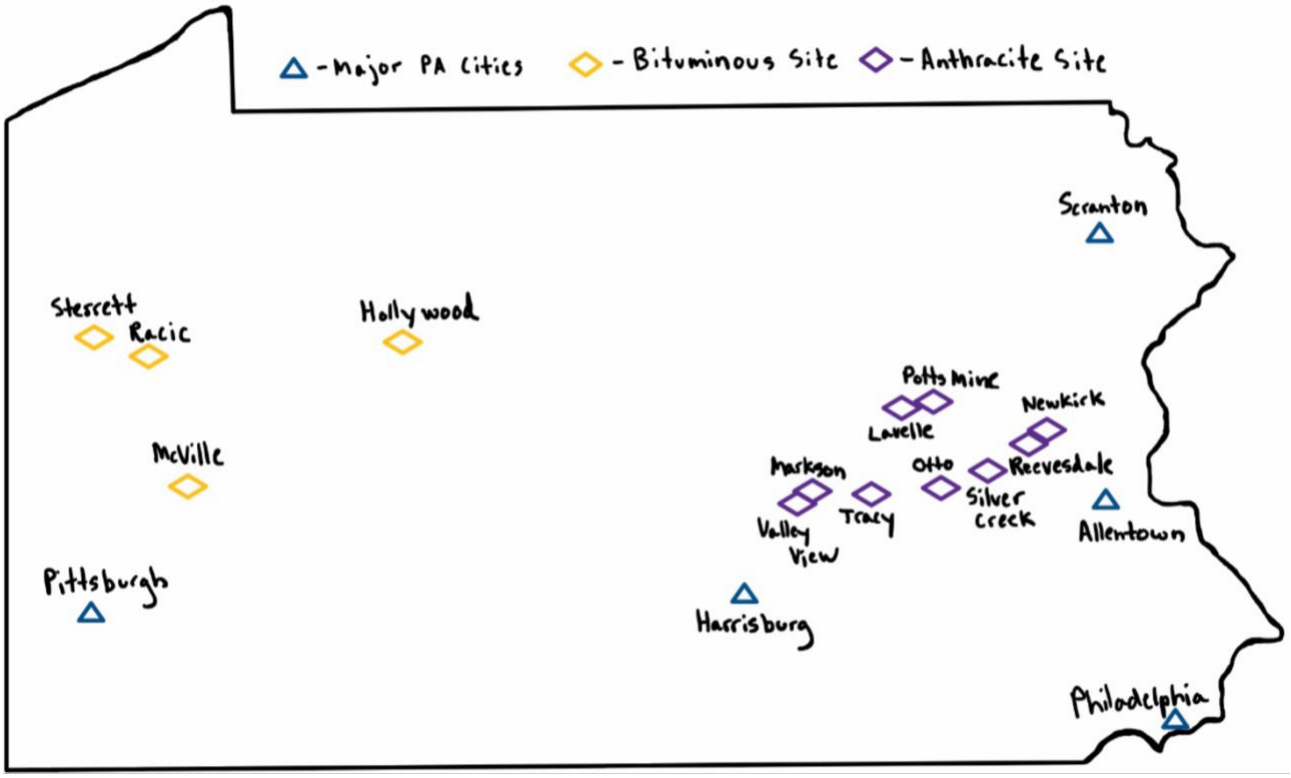

Figure 3: Map of Pennsylvania marking where all AMD samples were collected with the anthracite samples all being from eastern PA and the bituminous from western PA.

Lab Analysis Methods

Alkalinity analyses were done on each water sample via titration and reported as mg/L of $CaCO_3$. Cation testing was done using inductively coupled plasma-optical emission spectroscopy (ICP-OES). Similarly, anions were measured via ion chromatography methods (IC). Rare earth elements and trace metals were sent to the Penn State Laboratory for Isotopes and Metals in the Environment (LIME) for inductively coupled plasma-mass spectroscopy (ICP-MS) analyses.

Sediments were initially dried in an oven at 60 degrees Celsius until all moisture was completely removed. Upon drying, each sample was broken down in a mortar and pestle and separated through a 1.18-mm sieve. Fine sediments were packed into 20 mL HDPE liquid scintillation vials and wrapped in parafilm. Each scintillation vial was incubated for 21 days to allow for radium-226 daughter products (609, 295, and 351 keV) to grow in. Following incubation, the sediment was analyzed on a small anode Canberra gamma ray spectrometer for both radium-226 and 228 (911 keV peak).

Figure 4: Sediment after being dried in an oven (left). AMD samples packed in 20 mL scintillation vials to be analyzed on a Canberra gamma ray spectrometer (right).

After initial gamma data was recorded, the sediment from each scintillation vial was sent through an operationally defined four-step sequential leaching process. In order to target soluble salts, the first step only involved introducing the sediment samples to approximately 200 mL of Milli-Q ultrapure water. Once in solution, each sample was placed on a shaker for 24 hours, centrifuged for 20 minutes, and filtered through 0.45-micron nylon filters to separate the leachate from the sediment. The remaining sediment was freeze-dried at -46 degrees Celsius for 24-48 hours before being analyzed for radium-226 and 228 activity. The pH of each leachate sample was recorded before being stored in a lab refrigeration unit at 4 degrees Celsius. Following the Milli-Q solution, each sample was subjected to 1M ammonium acetate solution to separate exchangeable cations in clays. The process follows that described above, however the samples were only placed in a shaker for 12 hours and were given three consecutive washes

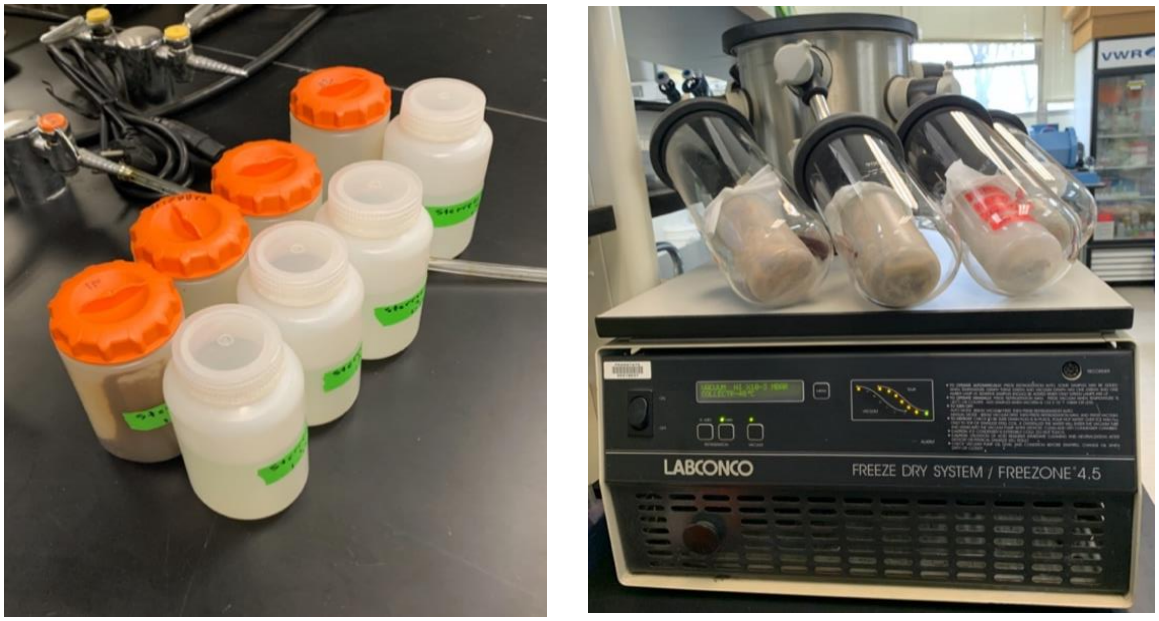

Figure 5: Centrifuged AMD sediment with naphthalene storage bottles containing leachate (left). Labconco Freezone 4.5 freeze dry system utilized during leaching process (right).

with Milli-Q to remove any traces of the 1M ammonium acetate solution. Following the same procedure as step 2, the sediment was tested for carbonates in 8% acetic acid solution and finally placed in 0.1M hydrochloric acid to analyze oxides

Radium-226 and 228 activities in residues were measured after every step via the Canberra gamma ray spectrometer. Each sample was not given 21 days for incubation. Radium-226 was measured from the 186 keV peak by also subtracting out background uranium measured at the 63 keV peak. In the future, leachates from every step will be measured for cations via ICP-MS, ICP-AES or both by Penn State LIME.

Figure 6: Canberra gamma ray spectrometer in Warner SALTS Laboratory.

Chapter 3 – Results and Discussion

Water Chemistry Data

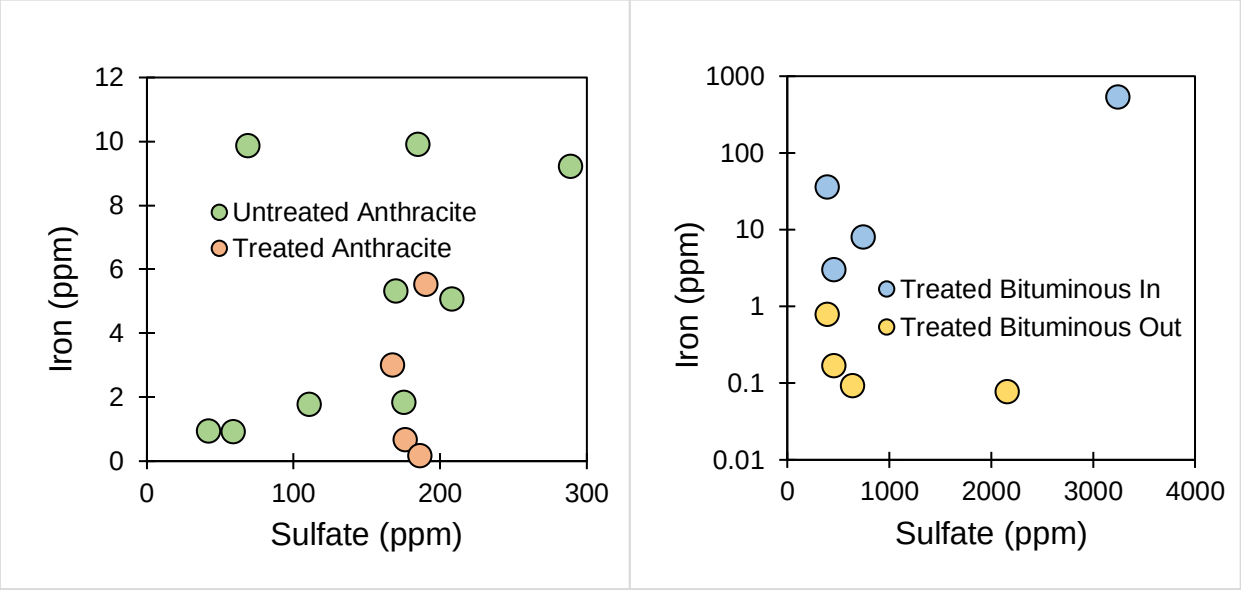

Figure 7: Iron concentration as a function of sulfate concentration in ppm for treated and untreated anthracite water samples (left). Iron concentration as a function of sulfate concentration in ppm for bituminous water samples into and out of treatment (right).

Based on the data shown in Figure 7, there were no noticeable trends in iron concentration as sulfate concentrations increased for both treated and untreated anthracite samples. However, iron concentrations were generally lower in treated samples when compared to their untreated counterparts. For the bituminous sample set, a majority of the iron concentrations were present at lower concentrations of sulfate. The iron concentrations of bituminous samples significantly decreased upon treatment from a high of 531.5 ppm of iron

before treatment to a low of 0.1 ppm of iron after treatment. All anthracite water samples were either untreated or passively treated via wetlands while the bituminous water samples were all actively treated with limestone.

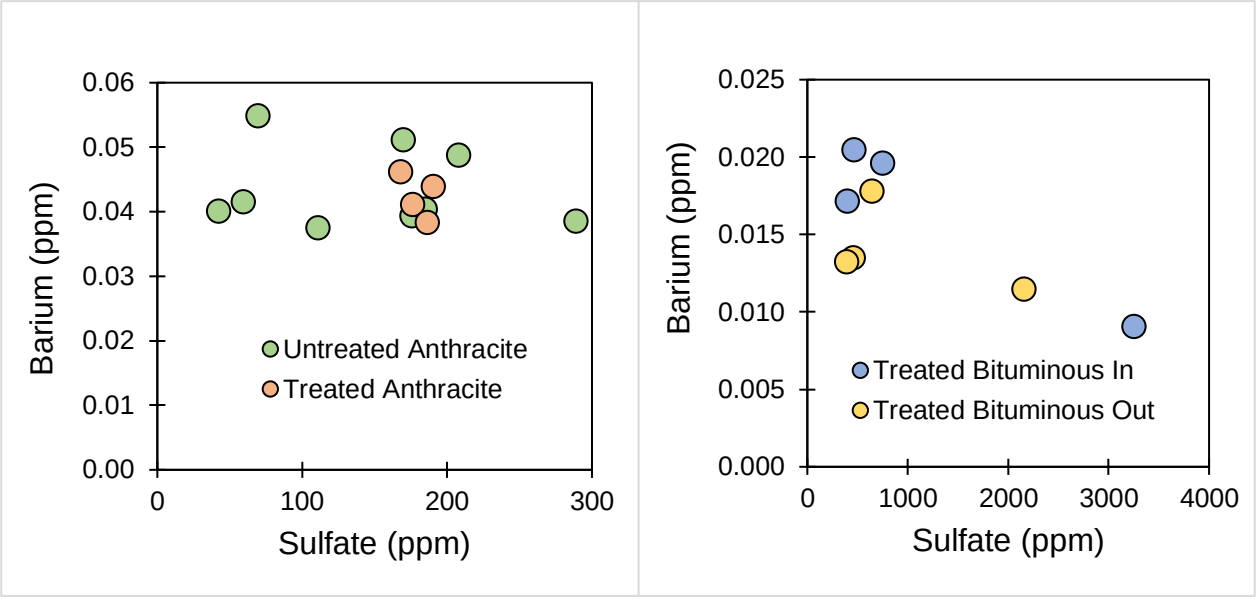

Figure 8: Barium concentration as a function of sulfate concentration in ppm for treated and untreated anthracite water samples (left). Barium concentration as a function of sulfate concentration in ppm for bituminous water samples into and out of treatment (right).

Anthracite water samples showed no obvious differences in barium concentration between treated and untreated samples as shown in Figure 8. The concentrations of barium also did not change drastically as the concentration of sulfate increased. The concentrations of barium in bituminous samples were generally lower in samples after treatment when compared to the same samples before treatment. A slightly negative correlation in barium concentration was observed as sulfate concentration increased for bituminous samples only. Overall, anthracite water samples had higher concentrations of barium than all other bituminous samples with the *lowest* barium concentration for anthracite being 0.037 ppm and the *highest* concentration for

bituminous samples being only 0.020 ppm. However, the concentration of sulfate for bituminous samples was consistently higher than that of all anthracite samples.

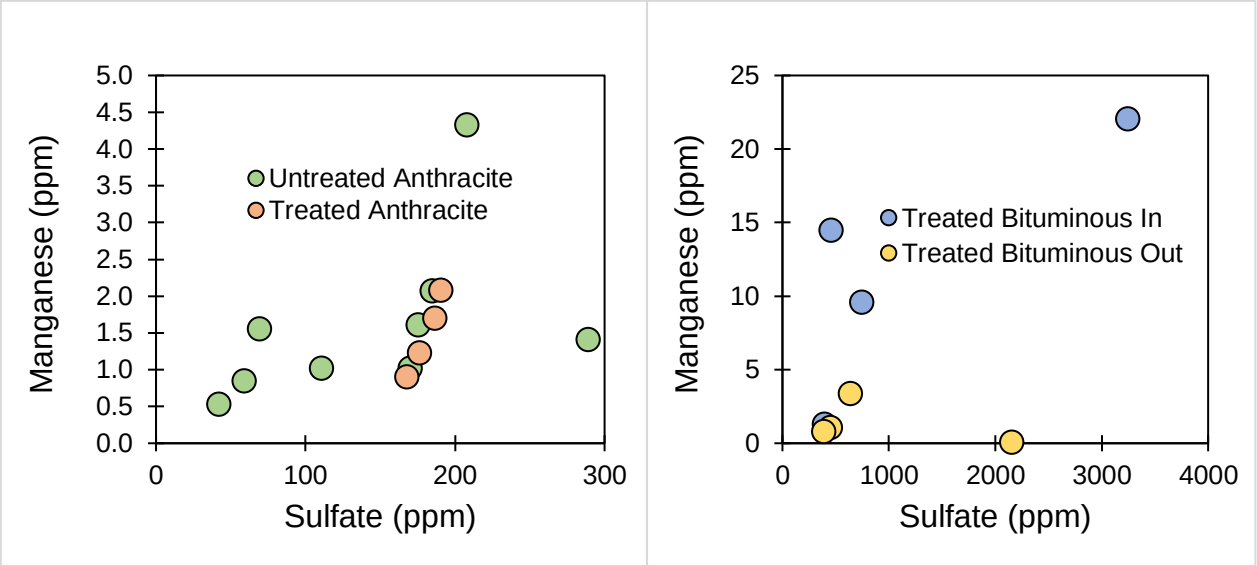

Figure 9: Manganese concentration as a function of sulfate concentration in ppm for treated and untreated anthracite water samples (left). Manganese concentrations as a function of sulfate concentration in ppm for bituminous water samples into and out of treatment (right).

As seen in Figure 9, the concentration of manganese did not clearly increase or decrease as the concentration of sulfate increased for anthracite samples. There is also no clear trend related to the concentration of manganese as sulfate increases for bituminous samples. Yet, the concentration of manganese in bituminous samples generally decreased after treatment with the highest concentration of manganese before treatment being 22 ppm and the lowest after treatment being 0 ppm.

Table 1: Water chemistry data for both untreated (green) and treated (orange) anthracite samples.

Sample	Temp, C	Conductance (SC25, µS/cm)	DO%	DO, mg/L	pH	pHmV	ORP (mV)	EhmV
Potts Mine E Branch	12.70	909	88.5	9.34	6.64	10.7	-129.9	81
Lavelle	9.77	283	16.9	1.94	3.6	163.5	513.9	728
Markson	11.00	517	46.8	5.16	3.99	144.4	449.0	661
Valley View	11.09	225	45.6	5.00	5.81	51.9	300.0	512
Newkirk_influent	9.20	300	93.8	10.79	3.99	143	514.0	728
Reevesdale	10.75	114	52.8	5.89	4.93	96.6	414.0	627
Otto In	12.04	442	67.0	7.19	5.95	45.8	294.0	505
Silvercreek In	11.95	486	13.0	1.40	5.86	49.7	245.0	457
Tracy	11.22	511	21.7	2.40	5.97	44.2	284.0	496
Otto Out	16.55	439	95.2	9.28	6.5	17.8	267.8	475
Silvercreek Out	20.36	472	97.3	9.32	7.22	-19.3	240.0	443
Silvercreek Cell 3 Out	15.96	494	91.0	8.98	6.67	88	208.0	416
Tracy Wetland	12.23	501	67.2	7.13	6.27	28.9	277.0	488

As shown in Table 1, water samples taken before and after treatment in sites such as Otto, Silvercreek, and Tracy yielded sizeable increases in pH after treatment. The most notable change in pH occurred in Silvercreek samples with a change from 5.86 to 7.22 between untreated and treated samples respectively. In these same sample sets, the concentration of dissolved oxygen increased greatly with the most significant change also occurring in Silvercreek samples with the concentration of dissolved oxygen increasing from 1.40 mg/L before treatment to 8.98 mg/L after treatment. Conductance values slightly decreased after treatment for all three of the Silvercreek, Otto, and Tracy sample sets. All ORP, pHmV, and EhmV values also slightly decreased upon treatment for the same sample sets with pHmV decreasing the most drastically after treatment in sites such as Silvercreek, which experienced the largest drop of 49.7 to -19.3.

Table 2: Water chemistry data for bituminous samples going into (blue) and out of (yellow) treatment.

Sample	Temp, C	Conductance (SC25, µS/cm)	DO%	DO, mg/L	pH	ORP (mV)	EhmV
Racic In	0.1	1875	0.0	N/A	2.97	539	762
Sterrett In	9.7	924	42.5	4.9	3.55	424	638
McVille in	3.3	4635	33.9	4.3	3.01	398	619
Hollywood in	8.7	869	64.1	7.4	3.28	422	637
Racic Out	1.0	1466	109.9	15.9	6.15	359	582
Sterrett DLB S Out	6.0	1048	29.1	3.6	6.89	174	392
McVille out	3.2	3402	92.7	12.3	9.28	158	379
Hollywood out	4.4	824	80.5	10.5	6.43	194	414

The pH of all bituminous samples increased upon treatment with the largest increase occurring in the McVille sample set with an increase from 3.01 to 9.28 as shown in Table 2. The concentration of dissolved oxygen also increased by a significant amount for each sample with an extremely large increase occurring in the Racic sample set from essentially 0 (N/A meaning the concentration was too low to get a reading) to 15.9 mg/L. ORP and EhmV values decreased for each sample upon treatment while conductance also decreased for all samples except for Sterrett where the conductance increased from 924 to 1048 µS/cm.

Sediment/Radium Data

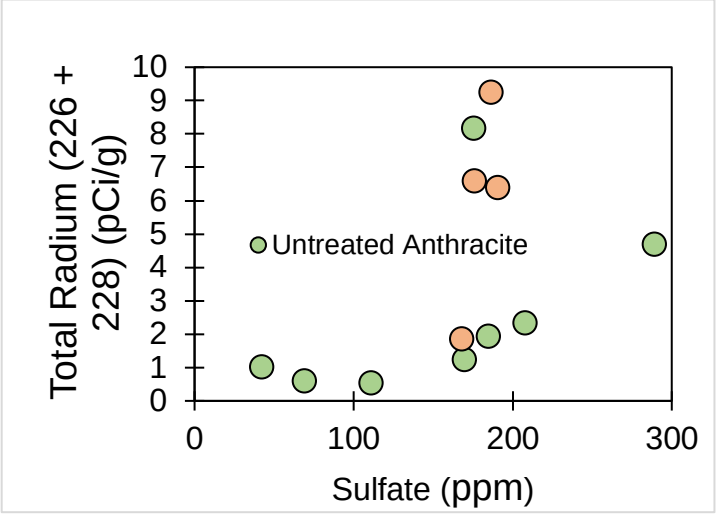

Figure 10: Total Radium as a function of sulfate concentration for untreated and treated anthracite sediment samples.

The total concentration of radium (pCi/g) in associated anthracite sediment samples represents the sum of radium-226 and radium-228. Untreated sediment samples generally had lower concentrations of total radium when compared to the corresponding treated samples as depicted in Figure 10. The highest reported concentration of total radium in untreated anthracite sediment was 8.17 pCi/g while the lowest was 0.60 pCi/g. In treated anthracite sediment, the highest concentration of total radium was observed at 9.23 pCi/g whereas the lowest concentration was 1.84 pCi/g.

A set of bituminous sediment samples from the same site (Sterrett) had significantly higher total radium concentrations than any of the anthracite samples shown in Figure 10 with the highest concentrations being 23.65, 17.09, 16.34, and 15.29 pCi/g respectively. Another set of bituminous sediment samples (McVille) had consistently lower total radium concentrations than all of the other anthracite samples shown above with recorded concentrations of 0.20, 0.09, and 0.04 pCi/g respectively.

Discussion of Radium Data

A study done on the natural radioactivity level of stone coal-bearing strata in East China observed the radioactivity of ^{238}U, ^{232}Th, ^{226}Ra, and ^{40}K radionuclides in air, solid, water, and plant media in regions typically associated with stone coal-bearing layers[6]. Via a subset set of 146 solid samples, the study found that the concentration of radium-226 in assorted sediment samples was averaged to 58.7 +/- 52.7 Bq/kg. If this value is converted to pCi/g in order to be compared to the data above, the results are 1.59 +/- 1.42 pCi/g[6]. This concentration corresponds to the lower-end of the spectrum for anthracite coal regions in PA with the lowest concentrations for treated and untreated anthracite samples being 1.84 and 0.60 pCi/g respectively. The lowest recorded concentrations for bituminous sediment samples in PA were from the McVille site with values such as 0.20, 0.09, and 0.04 pCi/g.

Another study was done on natural radioactivity levels in coal and coal combustion residues at a coal-based thermoelectric plant in Bangladesh. This study focused on the same radionuclides as the report from East China: ^{238}U, ^{232}Th, ^{226}Ra, and ^{40}K[7]. It was reported that the mean radium-226 concentration in feed coal samples was 41.7 +/- 18.2 Bq/kg or 1.13 +/- 0.49 pCi/g[7]. Similar to the study from East China, this value relates more closely to the lower spectrum for both untreated/treated anthracite and bituminous samples. The coal combustion residue had a much higher mean concentration of radium-226 at 140.5 +/- 28.4 Bq/kg or 3.80 +/- 0.77 pCi/g. While this concentration is higher than the feed coal samples, it is still relatively low compared to the radium-226 concentrations in AMD sediments from Pennsylvania.

Leaching Analysis

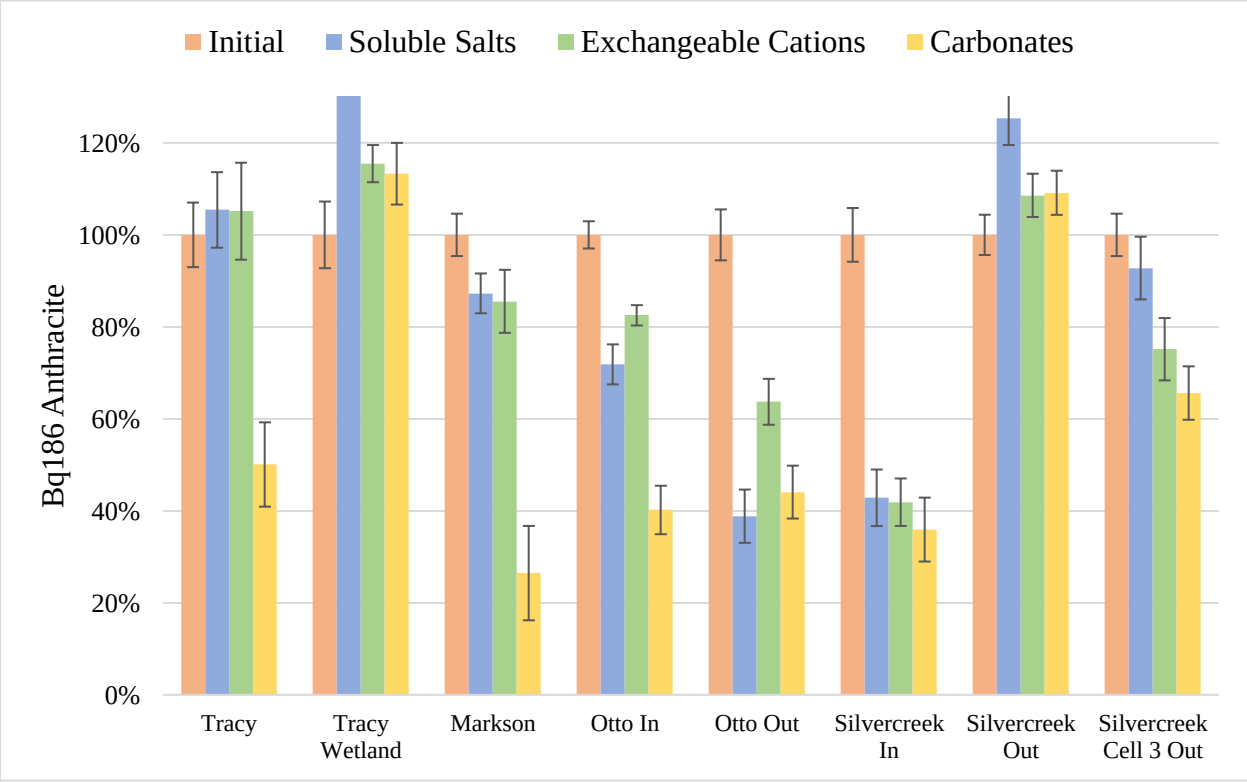

Figure 11: Radium concentration associated with each step of the sequential leaching process for anthracite sediment samples only. Each concentration relates to the 186 peak for radium-226 in Bq.

According to Figure 11, the most significant loss of radium-226 in anthracite sediment data was experienced in the following samples: Otto In, Otto Out, and Silvercreek In. Otto In still maintained approximately 70 percent of radium-226 after the first step, and ultimately held only 40 percent after the third leaching step that targets carbonates. Otto Out and Silvercreek In experienced much more significant drops in radium-226 after only the first step that targets soluble salts down to approximately 40 percent. In both cases, the level of radium-226 was maintained at approximately 40 percent of the initial radium-226 after the third step of the leaching process. Samples such as Tracy and Markson experienced nearly all of their corresponding decreases in radium-226 following the third step. Silvercreek Cell 3 Out showed a

constant drop in radium following each leaching step. Both Tracy Wetland and Silvercreek Out showed no loss of radium-226 after the first three steps.

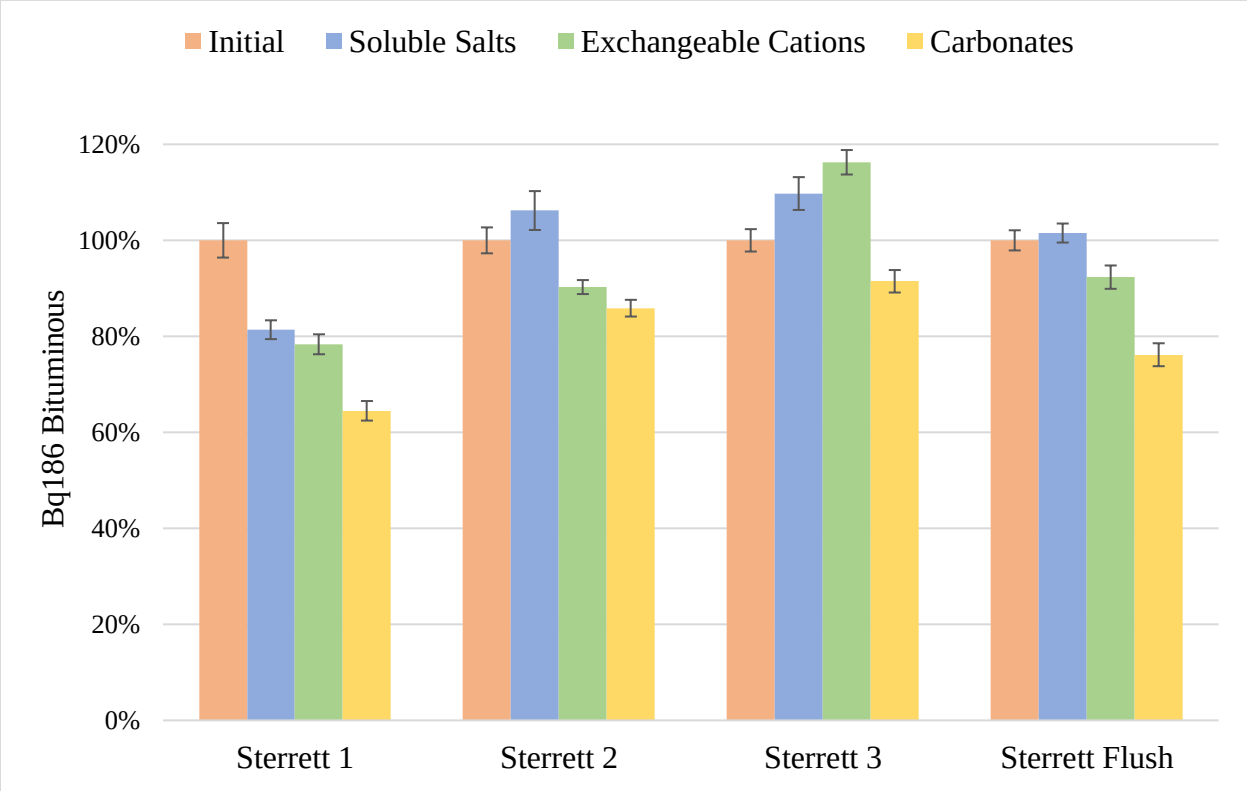

Figure 12: Radium concentration associated with each step of the sequential leaching process for bituminous sediment samples only. Each concentration relates to the 186 peak for radium-226 in Bq.

For bituminous sediment data sets, all samples maintained most of the initial radium-226 through the first three leaching steps. Sterrett 1 showed the largest decrease in radium-226 down to approximately 60 percent after the third step. The other corresponding bituminous sediment data sets maintained most of the initial radium-226 where the most significant drop was shown in Sterrett Flush out of the remaining samples. 76 percent of the radium still persisted in Sterrett Flush after the third step. Despite all of these samples showing only slight decreases in radium-226, all of these samples collectively lost the most sediment mass following step three. Sterrett 3 lost the most mass of any sample across both bituminous and anthracite sets at 4.4 grams. Sterrett

Flush lost the least of any bituminous sample with 2.6 grams, which is still higher than any anthracite sample set after step three.

Table 3: Radium data from 186 peak for all leached samples. Displayed in both Bq and pCi.

	Bq186			pCi186		
Sample	**Step 1**	**Step 2**	**Step 3**	**Step 1**	**Step 2**	**Step 3**
Tracy	0.180	0.180	0.086	5.406	4.583	2.140
Tracy Wetland	0.390	0.192	0.188	10.050	5.566	5.272
Markson	0.289	0.283	0.087	7.983	7.165	1.487
Otto In	0.551	0.633	0.308	14.155	18.186	9.409
Otto Out	0.270	0.442	0.306	7.998	11.940	8.872
Silvercreek In	0.091	0.089	0.076	2.367	3.026	1.832
SilverCreek Out	0.936	0.811	0.815	24.348	21.536	21.927
SilverCreek Cell 3 Out	0.553	0.448	0.391	13.730	11.014	10.712
Sterrett 1	1.919	1.847	1.521	52.620	49.603	41.520
Sterrett 2	2.528	2.149	2.044	67.576	59.041	55.186
Sterrett 3	1.950	2.066	1.625	52.071	55.404	43.785
Sterrett Flush	2.291	2.083	1.719	62.448	56.535	46.337
Racic 2	0.096	No Data	No Data	2.509	No Data	No Data
McVille 1(1)	0.325	No Data	No Data	8.122	No Data	No Data
McVille 3	0.113	No Data	No Data	3.049	No Data	No Data

All of the exact radium-226 concentrations (from the 186 peak) for each step are shown above. Racic 2, McVille 1 (1), and McVille 3 were all excluded from the study since there was such a negligible amount of radium-226 present after the first step. Likewise, these data sets took extremely long to run on the gamma ray spectrometer due to this miniscule amount of radium activity, further increasing the likelihood that these samples would be void. This table also shows the relative amounts of radium-226 in pCi for the total mass of each sample. While the 911 peak for radium-228 was not explicitly graphed, a similar table can be found in Appendix B showing

the concentrations of radium-228 from each sample following each step of the sequential leaching process in both Bq and pCi.

Chapter 4 – Conclusion

Due to the social limitations imposed by the novel coronavirus, the fourth and final leaching step was not able to be conducted. The final step of the sequential leaching process separates manganese and iron oxides from the total sediment mass. Therefore, for the purpose of this research project, it can be assumed that sediment samples with most or all of the initial radium still contained within the sediment after the first three steps would either have most of the radium either adsorbed by manganese and iron oxides or co-precipitated with sulfate minerals such as barium. This final leaching step can be completed once the social limitations imposed to control the spread of the coronavirus are lifted and lab research can continue.

Radium that is removed during step four would indicate that the radium was adsorbed by iron and manganese oxides. If most of the radium still persists within the sediment after the fourth step, then it would be an indication that the radium was co-precipitated with barium and sulfate as radiobarite.

It was initially expected that samples high in iron and manganese, such as sediment from anthracite and bituminous coal regions, would have radium primarily adsorbed by these minerals rather than co-precipitated with barium. Anthracite samples such as Tracy Wetland and Silvercreek Out lost no radium across the first three steps. Both of these samples were passively treated and had higher concentrations of manganese and iron collectively than barium. Tracy Wetland and Silvercreek Out had concentrations of 0.90 and 1.69 ppm for manganese and 2.99

and 0.15 ppm for iron respectively. Their corresponding barium concentrations were 0.046 and 0.038 ppm respectively. Therefore, it is assumed that both samples would have a majority of the radium removed after the final leaching step.

Similar to the anthracite samples, the Sterrett sample sets collectively had higher concentration of manganese and iron when compared to barium. Iron concentrations were approximately 0.17 ppm while the manganese concentrations were somewhat higher at 1.1 ppm. However, the concentration of barium in Sterrett samples was very low at 0.013 ppm. The large decrease in sediment mass experienced across the Sterrett sediment samples during the carbonate step of the leaching process most likely stems from the fact that they were all actively treated with limestone. Yet, since the concentration of barium was extremely low, it is also likely that most of the radium-226 present in these samples would have been removed after the fourth leaching step that targets iron and manganese oxides.

It was originally suspected that sediment from coal mining regions such as eastern and western Pennsylvania would have higher concentrations of manganese and iron oxides than barium. As shown by the data presented in this document, that hypothesis held true. Due to social limitations, the leaching step that would have proven that most of the radium associated with the sediment samples would have been removed with the final leaching step that targets iron and manganese oxides could not be conducted. Regardless, the low barium concentrations relative to iron and manganese in all samples suggests that radium would most likely be adsorbed by iron and manganese molecules rather than being co-precipitated with barium and sulfate as radiobarite.

Appendix A – Significant Figures

Figure 3

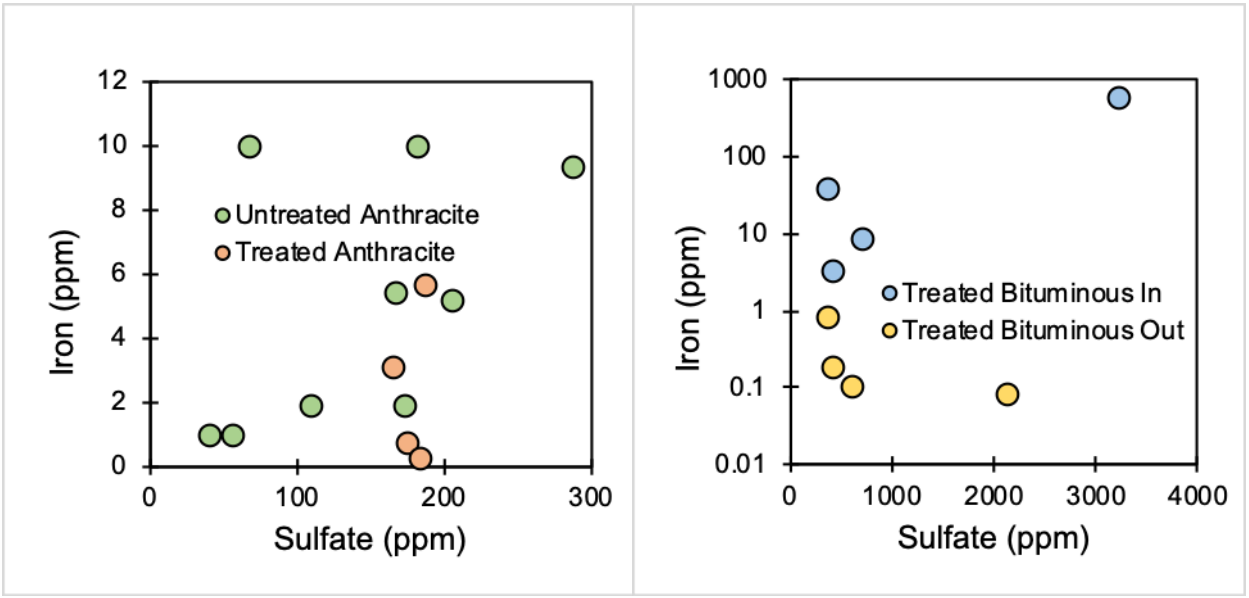

Figure 7

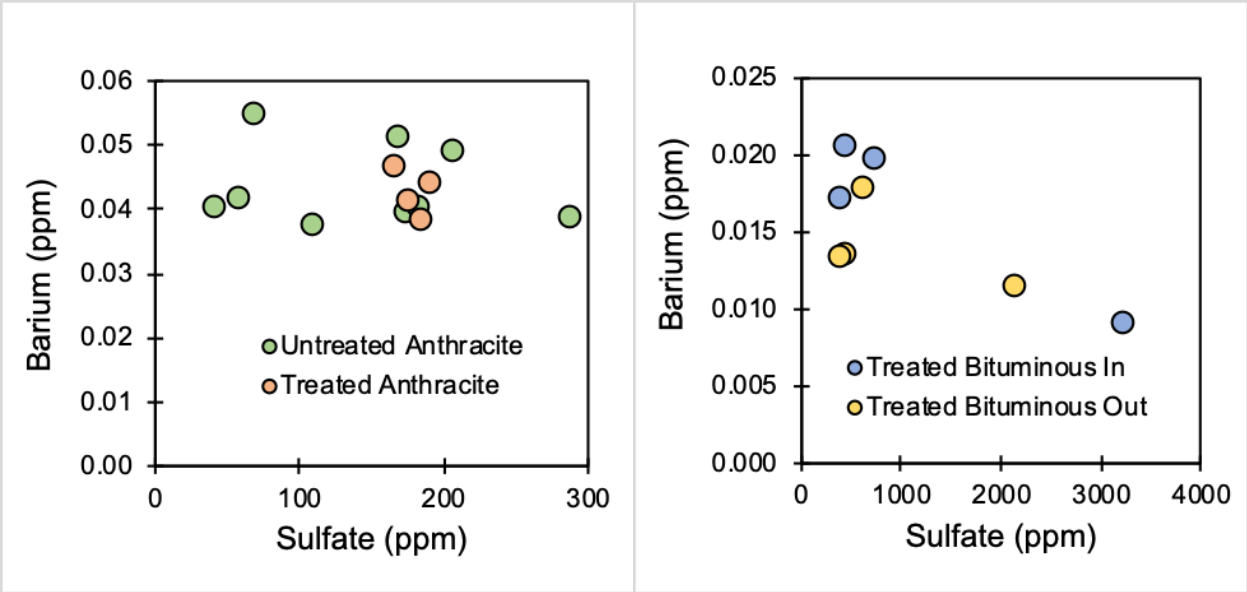

Figure 8

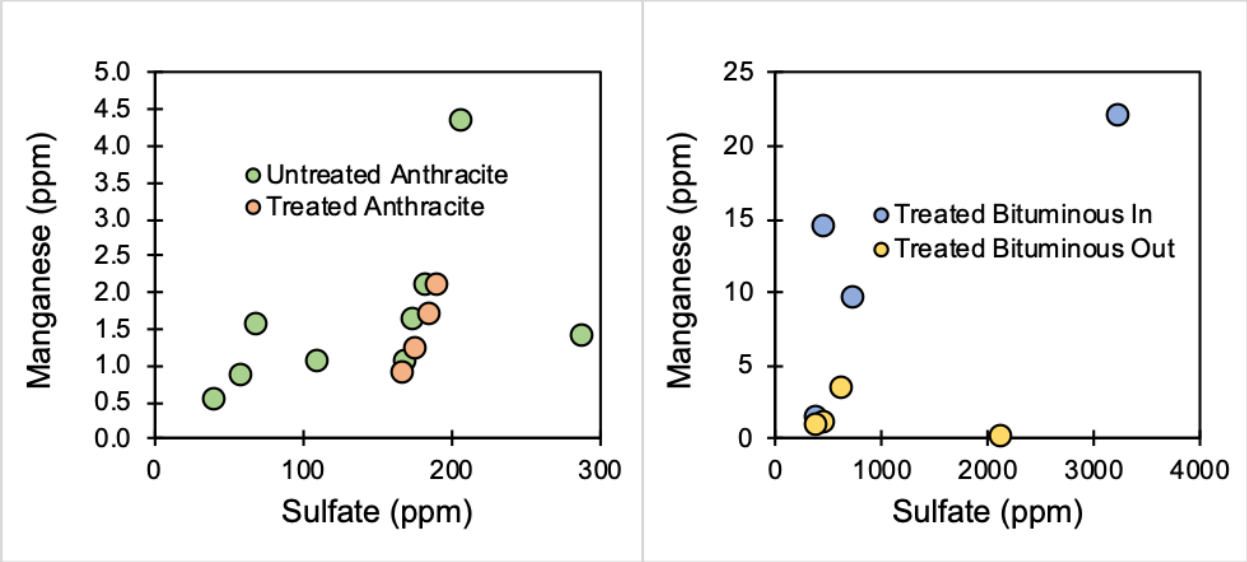

Figure 9

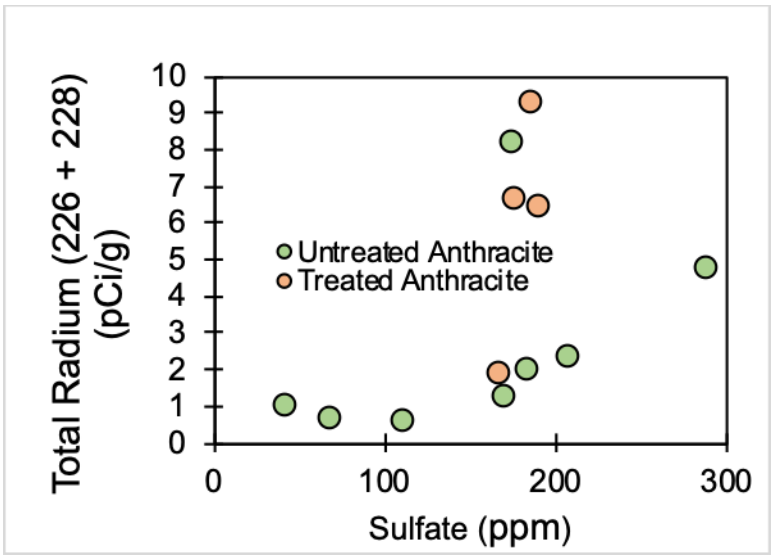

Figure 10

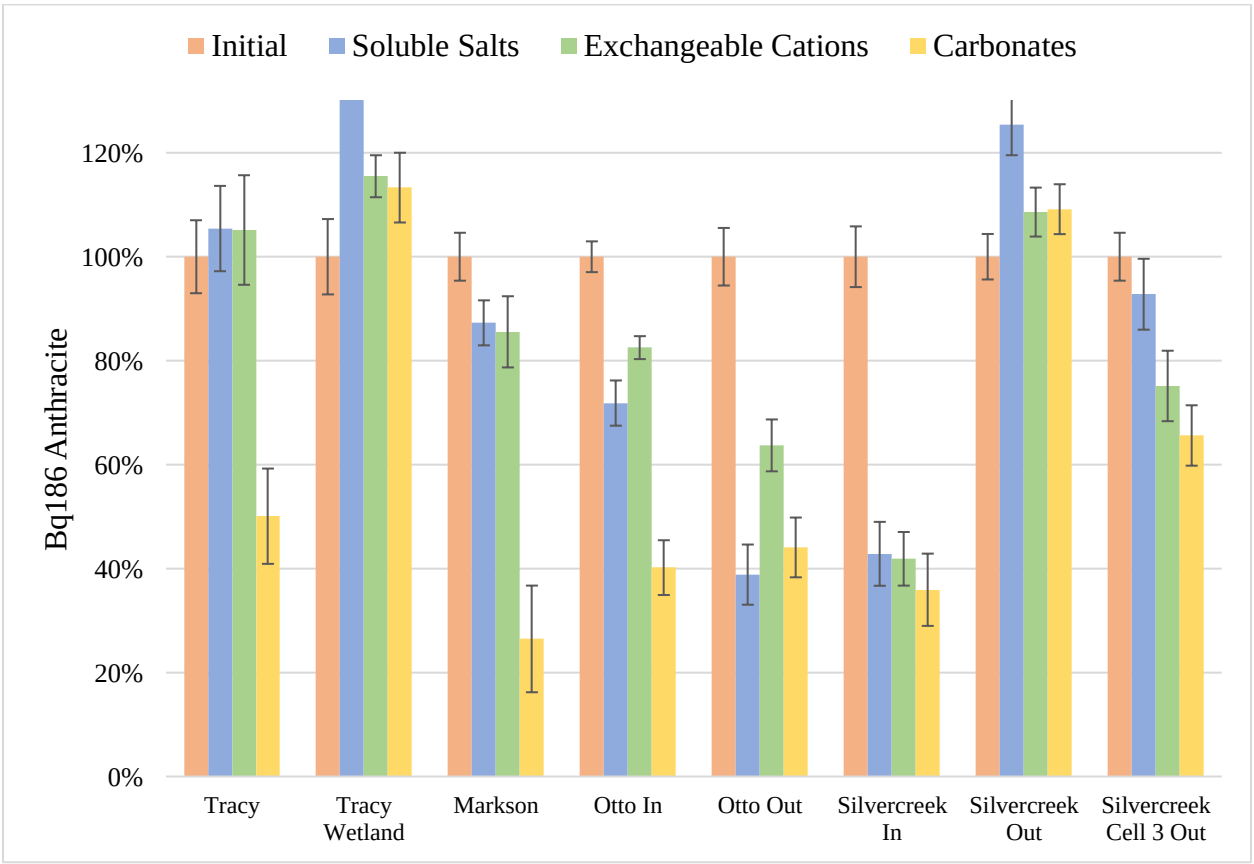

Figure 11

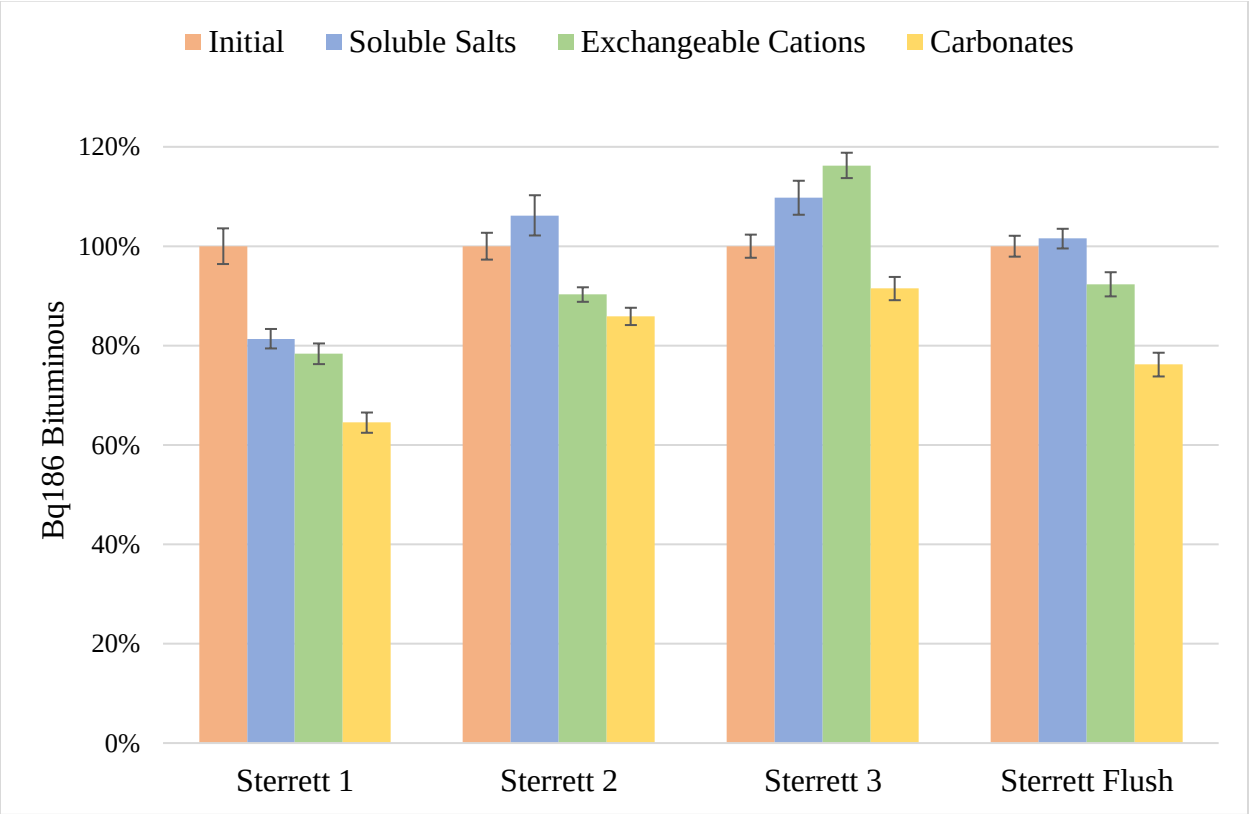
Initial
Soluble Salts
Exchangeable Cations
Carbonates
120%
100%
80%
60%
40%
20%
0%
Bq186 Bituminous
Sterrett 1
Sterrett 2
Sterrett 3
Sterrett Flush

Figure 12

Appendix B – Significant Tables

Table 1

Sample	Temp, C	Conductance (SC25, µS/cm)	DO%	DO, mg/L	pH	pHmV	ORP (mV)	EhmV
Potts Mine E Branch	12.70	909	88.5	9.34	6.64	10.7	-129.9	81
Lavelle	9.77	283	16.9	1.94	3.6	163.5	513.9	728
Markson	11.00	517	46.8	5.16	3.99	144.4	449.0	661
Valley View	11.09	225	45.6	5.00	5.81	51.9	300.0	512
Newkirk_influent	9.20	300	93.8	10.79	3.99	143	514.0	728
Reevesdale	10.75	114	52.8	5.89	4.93	96.6	414.0	627
Otto In	12.04	442	67.0	7.19	5.95	45.8	294.0	505
Silvercreek In	11.95	486	13.0	1.40	5.86	49.7	245.0	457
Tracy	11.22	511	21.7	2.40	5.97	44.2	284.0	496
Otto Out	16.55	439	95.2	9.28	6.5	17.8	267.8	475
Silvercreek Out	20.36	472	97.3	9.32	7.22	-19.3	240.0	443
Silvercreek Cell 3 Out	15.96	494	91.0	8.98	6.67	88	208.0	416
Tracy Wetland	12.23	501	67.2	7.13	6.27	28.9	277.0	488

Table 2

Sample	Temp, C	Conductance (SC25, µS/cm)	DO%	DO, mg/L	pH	ORP (mV)	EhmV
Racic In	0.1	1875	0.0	N/A	2.97	539	762
Sterrett In	9.7	924	42.5	4.9	3.55	424	638
McVille in	3.3	4635	33.9	4.3	3.01	398	619
Hollywood in	8.7	869	64.1	7.4	3.28	422	637
Racic Out	1.0	1466	109.9	15.9	6.15	359	582
Sterrett DLB S Out	6.0	1048	29.1	3.6	6.89	174	392
McVille out	3.2	3402	92.7	12.3	9.28	158	379
Hollywood out	4.4	824	80.5	10.5	6.43	194	414

Table 3

Sample	Bq186			pCi186		
	Step 1	**Step 2**	**Step 3**	**Step 1**	**Step 2**	**Step 3**
Tracy	0.180	0.180	0.086	5.406	4.583	2.140
Tracy Wetland	0.390	0.192	0.188	10.050	5.566	5.272
Markson	0.289	0.283	0.087	7.983	7.165	1.487
Otto In	0.551	0.633	0.308	14.155	18.186	9.409
Otto Out	0.270	0.442	0.306	7.998	11.940	8.872
Silvercreek In	0.091	0.089	0.076	2.367	3.026	1.832
SilverCreek Out	0.936	0.811	0.815	24.348	21.536	21.927
SilverCreek Cell 3 Out	0.553	0.448	0.391	13.730	11.014	10.712
Sterrett 1	1.919	1.847	1.521	52.620	49.603	41.520
Sterrett 2	2.528	2.149	2.044	67.576	59.041	55.186
Sterrett 3	1.950	2.066	1.625	52.071	55.404	43.785
Sterrett Flush	2.291	2.083	1.719	62.448	56.535	46.337
Racic 2	0.096	No Data	No Data	2.509	No Data	No Data
McVille 1(1)	0.325	No Data	No Data	8.122	No Data	No Data
McVille 3	0.113	No Data	No Data	3.049	No Data	No Data

Table 4

Sample	Bq911			pCi911		
	Step 1	**Step 2**	**Step 3**	**Step 1**	**Step 2**	**Step 3**
Tracy	0.180	0.270	0.086	5.316	7.279	1.712
Tracy Wetland	0.390	0.288	0.282	11.709	8.253	8.003
Markson	0.385	0.283	0.262	10.676	7.259	7.612
Otto In	2.574	2.443	2.545	70.682	66.954	67.710
Otto Out	1.797	1.857	1.683	48.888	49.175	45.277
Silvercreek In	0.364	0.356	0.305	10.741	9.878	8.244
SilverCreek Out	2.341	2.433	2.364	62.182	66.139	63.824
SilverCreek Cell 3 Out	1.751	1.701	1.486	46.811	46.207	40.190
Sterrett 1	4.545	4.341	4.364	123.521	117.681	117.617
Sterrett 2	5.639	5.605	5.678	152.751	150.685	154.147
Sterrett 3	3.218	3.193	2.692	86.102	87.426	73.450
Sterrett Flush	3.386	3.030	2.956	90.933	81.915	79.336
Racic 2	0.675	0.64498	No Data	19.489	17.78302	No Data
McVille 1(1)	0.108	No Data	No Data	1.841	No Data	No Data
McVille 3	0.000	No Data	No Data	0.000	No Data	No Data

BIBLIOGRAPHY

1) Cravotta III, C. “Dissolved metals and associated constituents in abandoned coal-mine discharges, Pennsylvania, USA. Part 1: Constituents quantities and correlations” *Applied Geochemistry*. 2008, 23, 2, 166-202

2) Johnson, B., Hallberg, K. “Acid mine drainage remediation options: a review.” *Science of The Total Environment*. 2005, 338, 1-2, 3-14

3) McDevitt, B., et al. “Emerging Investigator series: radium accumulation in carbonate river sediments at oil and gas produced water discharges: implications for beneficial use as disposal management” *Environmental Science: Processes & Impacts*. 2019, 2

4) Udayabhanu, G. and Prasad, B. “Studies on Environmental Impact of Acid Mine Drainage Generation and its Treatment: An appraisal.” *Indian Journal of Environmental Protection.* 2010, 30. 11. 953-967

5) Sice, K., et al. “Radium attenuation and mobilization in stream sediments following oil and gas wastewater disposal in western Pennsylvania” *Applied Geochemistry.* 2018, 98, 393-403

6) Xu, N., Wei, X., Kuang, F. et al. “Study on the natural radioactivity level of stone coal-bearing strata in East China.” *Environ Earth Sci*. 2018, 77. 726

7) Habib, Md A., et al. "Assessment of Natural Radioactivity in Coals and Coal Combustion Residues from a Coal-Based Thermoelectric Plant in Bangladesh: Implications for Radiological Health Hazards." *Environmental Monitoring and Assessment*. 2019, 191. 1. 1-20

ACADEMIC VITA

GARRETT REESE

greese2632@gmail.com

EDUCATION

B.S., Chemical Engineering (3.54 GPA)

U.M.N.R., Environmental Engineering Expected Graduation: May 2020

The Pennsylvania State University, Schreyer Honors College

EXPERIENCE

Process Engineering Intern, Carmeuse Lime and Stone May 2019 – August 2019

- Planned, designed, and implemented independent projects including two high temperature glass doors to improve kiln efficiency for an estimated savings of approximately $100,000 a year
- Oversaw weekly safety inspections to discover faulty equipment, false air leaks, and unsafe conditions
- Developed numerous calculators on Excel to streamline loss of ignition and lime quality testing, to determine approximate energy/fuel savings by reducing false air, and to predict an optimal fuel blend for day to day use
- Conducted LOI (loss of ignition) and available CaO tests, fuel moisture observations, and CO_2/sulfur testing on both dolomitic and hi-cal lime products while filling in as a lab technician

- Met contractors off-site to discuss the design of glass doors and to finalize costs
- Calculated air flow measurements, heat loss trends, and collected thermal imaging data

Summer Student, UGI Utilities – Electric Division June 2016 – January 2019

- Discussed newly designed projects with electrical/mechanical engineers and utility workers to ensure the correct materials were distributed and implemented properly
- Managed warehouse inventory and distributed material requested by UGI and Asplundh line crews
- Completed several small-scale construction operations such as laying tile and concrete, pulling wire, etc.
- Trained incoming employees

UNDERGRADUATE RESEARCH AND WORK

The Pennsylvania State University

CurtisLab (Chemical Engineering) August 2018 – December 2019

- Worked alongside of graduate students to genetically engineer seven constructs of chlorella that could reject sulfur particles specifically for use in an industrial setting such as the effluent stack of a coal-fired power plant
- Operated autoclave machines, pH readers, gel electrophoresis analysis software, centrifuges, etc.

SALTS Lab (Environmental Engineering) January 2019 – May 2020

- Packed gamma vials of sediment affected by natural gas wastewater, sand containing fecal matter from freshwater mussels, and soil affected by acid mine drainage taken from both northeastern and western Pennsylvania

- Currently writing a thesis on the accumulation of radium in acid mine drainage to determine the most prominent form of coprecipitation of barium with sulfate or manganese and iron oxides

Grader – CE 370 (Environmental Engineering) August 2019 – December 2019

- Graded papers, homework, etc. for a section of nearly 100 students on top of regular course work in ChE

Tutor – OXE August 2018 – May 2019

- Provided weekly homework help for introductory courses in chemical engineering (material balance and thermodynamics) and hosted resume review sessions

---

ACTIVITIES

Omega Chi Epsilon (OXE) - Chemical Engineering Honor Society August 2018 – May 2020

Honor Society May 2017 – May 2020

AIChE (American Institute of Chemical Engineers) August 2018 – May 2020

Habitat for Humanity January 2018 – December 2019